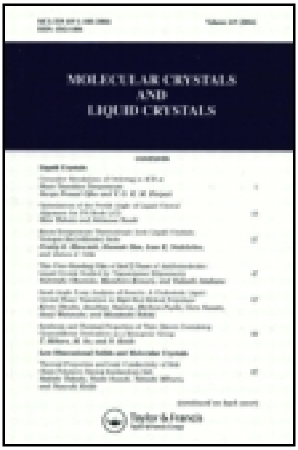

Molecular Crystals and Liquid Crystals Science and Technology. Section A. Molecular Crystals and Liquid Crystals
Publication details, including instructions for authors and subscription information:
http://www.tandfonline.com/loi/gmcl19

Intracrystalline Structure of Chromium Oxide-Cluster Pillar in Montmorillonite

Jin-Ho Choy [a], Jin-Tae Kim [a], Joo-Byoung Yoon [a] & Dong-Kuk Kim [b]

[a] Department of Chemistry, Center for Molecular Catalysis, Seoul National University, Seoul, 151-742, Korea

[b] Department of Chemistry, Kyungpook National University, Taegu, 702-701, Korea

To cite this article: Jin-Ho Choy, Jin-Tae Kim, Joo-Byoung Yoon & Dong-Kuk Kim (1998): Intracrystalline Structure of Chromium Oxide-Cluster Pillar in Montmorillonite, Molecular Crystals and Liquid Crystals Science and Technology. Section A. Molecular Crystals and Liquid Crystals, 311:1, 315-320

To link to this article: http://dx.doi.org/10.1080/10587259808042404

Mol. Cryst. Liq. Cryst., 1998, Vol. 311, pp. 315–320
Reprints available directly from the publisher
Photocopying permitted by license only

Intracrystalline Structure of Chromium Oxide-Cluster Pillar in Montmorillonite

JIN-HO CHOY[a], JIN-TAE KIM[a], JOO-BYOUNG YOON[a], and DONG-KUK KIM[b]
[a]Department of Chemistry, Center for Molecular Catalysis, Seoul National University, Seoul 151-742, Korea; [b]Department of Chemistry, Kyungpook National University, Taegu 702-701, Korea

Chromia pillared clay was prepared by ion exchange type intercalation reaction between Na^+-montmorillonite and the trimeric chromium oxyformate (TCF) salt in an aqueous solution. According to powder XRD, the basal spacing of 16.4 Å upon intercalation of TCF ion suggests that the Cr_3O plane is parallel to the aluminosilicate layers with a gallery height of ~6.8 Å. Even though the basal spacing decreases slightly upon heating, the layer structure is retained and beyond 400 °C it transforms into microporous Cr_2O_3 pillared montmorillonite with BET specific surface area of 152 m^2/g. XANES spectroscopy confirms that the trivalent chromium ion is stabilized in the interlayer space without any further oxidation to higher valence upon heat treatment. According to the EXAFS spectroscopic analysis, the Cr-Cr bond length (3.29 Å) of vertex-linkaged CrO_6 octahedron in the precursor TCF splits into 2.64 Å, 2.98 Å, and 3.77 Å during the calcination, due to the face-, edge-, and corner-linkaged CrO_6 octahedra, respectively, similar to the chromium oxide, Cr_2O_3.

Keywords: pillared clay; chromium; EXAFS; XANES

INTRODUCTION

There has been considerable interest in introducing robust materials such as metal oxides or chalcogenides into the interlamellar regions of swelling clays in order to keep the layers apart, thus resulting in the internal surface available for adsorption and possible catalysis.[1-3] Among various metal oxide pillared clays, the chromium oxide one is known to be a good catalyst for the dehydrogenation of cyclohexane.[4]

In the present work, an attempt was made to intercalate trimeric chromium oxyformate (TCF) ions, $[Cr_3O(HCO_2)_6(H_2O)_3]^+$, into the interlayer space of clay in order to keep the mineral layers apart at high temperature. We took use of Cr K-edge X-ray absorption spectroscopy (XAS) to prove some structural details and oxidation state of chromium species upon the pillaring.

For the characterization of pillared clay, we employed the EXAFS and XANES, since they are very useful in determining the electronic and geometric structures of layered materials. In this regard, we have previously carried out the structural studies on the copper complex intercalated layer silicates[5] and the organic alkoxide substituted FeOCl via EXAFS technique.[6]

EXPERIMENTAL SECTION

TCF was prepared as previously described,[7] and for the ion-exchange type intercalation reaction, montmorillonite was at first converted into the sodium form by treating it with 1N NaCl solution. These sodium saturated samples were then fractionated according to Stoke's law with a particle size below 2 μm. For the formation of TCF-intercalated montmorillonite (TCF-IM), montmorillonite was immersed into an aqueous TCF^+Cl^- solution at 65 °C for one week. The ion exchanged clay was centrifuged and washed until the Cl^- test became negative using $AgNO_3$ solution. Then TCF-IM was finally calcined at 400 °C (TCF-PILC400).

X-ray diffraction measurements were carried out with JEOL JDX-5P diffractometer (Ni filtered Cu Kα radiation (λ = 1.54184 Å). TG/DTA was performed with a Rigaku TAS 100 thermal analyzer in the temperature range from 25°C to 600 °C, with a heating rate of 10 °C/min under an ambient atmosphere. The specific surface area (BET) was determined with a Quantasorb sorption system. X-ray absorption spectra were recorded by using the synchrotron radiation EXAFS facilities installed at the beam line 7C in the Photon Factory (KEK, Tsukuba), operated at 2.5 GeV with ca. 260 ~ 370 mA of stored current. All the data were recorded in a transmission mode at room temperature. The intensities of incident and transmitted beams were measured with N_2- and (15 % Ar - 85 % N_2)-filled ionization chambers, respectively.

The analyses for experimental spectra were performed by the standard procedure as previously described.[8] The EXAFS spectra were k^3-weighted in order to compensate for the attenuation of EXAFS amplitude at high k, and then Fourier transformed in the range of $2.5\ \text{Å}^{-1} \le k \le 13.5\ \text{Å}^{-1}$ with a Hanning apodization function.

RESULTS AND DISCUSSION

Powder XRD analyses were carried out for the TCF-IM and its calcined derivatives at 250 °C and 400 °C, respectively. Even though the basal spacing decreases slightly from 16.4 Å to 15.8 Å upon heating, two-dimensional structure was retained as confirmed by the well developed (00ℓ) reflection. Such a result represents the pillaring process is topotatic. Beyond 400 °C, it transforms into microporous Cr_2O_3 pillared montmorillonite with specific surface area of 152 m^2/g. The basal spacing of 16.4 Å upon intercalation of TCF^+ ion suggests that Cr_3O plane is parallel to the layers of aluminosilicates with a gallery height of ~6.8 Å.

In order to evaluate the thermal stability of chromia pillared clay, TG/DTA measurement was carried out in an ambient atmosphere. Two significant weight losses in TG curve were found at around 112 °C and 367 °C. The first endothermic peak is due to removal of free water in the interlayer space and the second exothermic one was due to the decomposition of organic moiety of intercalated TCF^+ ion. No more thermal event could be observed beyond 400 °C, representing the pillaring process was already accomplished and powder XRD confirmed that the pillared clay is thermally stable up to 600 °C.

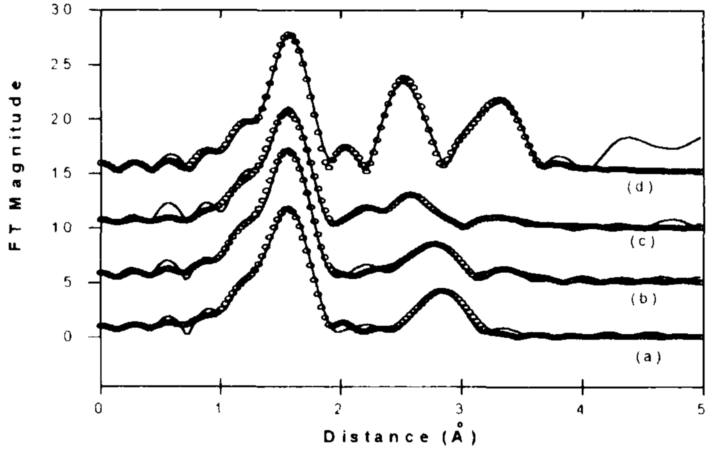

FIGURE 1 The k^3 weighted Fourier Transformed EXAFS spectra (solid line) and the fitting results (circle) for TCF^+Cl^- (a), TCF-IM (b), TCF-PILC400 (c), and Cr_2O_3 (d).

In order to examine the evolution of electronic and geometric structure of Cr in TCF-IM and TCF-PILC400, X-ray absorption measurements were carried out at the Cr K-edge. In the Cr K-edge XANES spectra of both compounds, the edge energies and pre-edge intensities were similar, indicating the conservation of the Cr^{3+} oxidation state. On the other hand, we could observe a significant shift of the peak around 6020 eV, which reflects the multiple scattering between the central atom and the second neighbors.[9] For the TCF-PILC400, the peak shifted to the higher energy by ~10 eV than that of TCF-IM. Such a result represents the decrease of the bond distance between Cr and second neighbors upon heat treatment.

In order to investigate more detailed structure and bonding character, EXAFS analysis was carried out at the Cr K-edge. The k^3-weighted EXAFS oscillation was Fourier transformed in the k range of 2.5 ~ 13.5 Å^{-1} (Figure 1). The FT magnitude (phase shift uncorrected) shows that the peak at ~2.9 Å due to Cr-Cr disappears with an appearance of new peaks at ~2.3 Å and ~2.6 Å upon heating. The non linear least-square curve fitting was carried out by using the theoretical standard[10] calculated from the structure of TCF^+Cl^-[11]. The best fitting results for TCF-IM and TCF-PILC400 are summarized in Table 1.

TABLE 1 The EXAFS fitting results for TCF-IM and TCF-PILC400.[a]

Compounds	Bond	Distance (Å)	N[a]	σ^2 (10^{-3}Å^{-2})[b]	E_0 shift (eV)[c]
TCF-IM	Cr-O	1.88	1	2.92	-1.00
	Cr-O	1.97	4	3.50	-1.00
	Cr-O	2.02	1	3.00	-1.00
	Cr-C	2.94	8	5.55	-4.20
	Cr-Cr	3.29	2	8.01	-4.23
TCF-PILC400	Cr-O	1.97	6.0	5.18	-2.39
	Cr-Cr	2.64	0.9	3.53	-9.23
	Cr-Cr	2.97	1.2	3.16	-6.26
	Cr-Cr	3.87	1.0	5.00	-4.52
Cr_2O_3	Cr-O	1.99	6.0	3.33	0.61
	Cr-Cr	2.66	1.0	5.73	-0.44
	Cr-Cr	2.91	3.0	3.30	-0.44
	Cr-Cr	3.42	3.0	3.04	-0.44
	Cr-Cr	3.66	6.0	5.57	-0.44

[a] Coordination number; [b] Debye-Waller factor; [c] threshold energy difference.

According to the EXAFS curve fitting results, the local structure around chromium in TCF-IM is identical with that of TCF^+Cl^-, indicating that the basic structure of TCF^+ ion was not altered by intercalation, but in case of TCF-PILC400, the Cr-Cr bond length (3.29 Å) of vertex-linkaged CrO_6 octahedron in the precursor TCF ion splits into 2.64 Å, 2.97 Å, and 3.87 Å upon heating, corresponding to face-, edge-, and corner-linkaged CrO_6 octahedra, respectively, similar to the chromium oxide, Cr_2O_3.[12]

Acknowledgments

The authors are grateful to Korea Ministry of Education for the support (BSRI-96-3413) and Prof. M. Nomura for his kind assistance at BL7C. J.-B. Yoon is grateful to Korea Research Foundation for his scholarship

References

[1.] T. J. Pinnavaia, *Science*, **220**, 365 (1988).
[2.] S. Yamanaka and M. Hattori, *Catalysis Today*, **2**, 261 (1988).
[3.] G. W. Brindley and S. Yamanaka, *Am. Mineral.*, **64**, 830 (1979).
[4.] T. J. Pinnavaia, M. S. Tzou, and S. D. Landau, *J. Am. Chem. Soc*, **107**, 4783 (1985).
[5.] J.-H. Choy, D.-K. Kim, J.-C. Park, S. N. Choi, Y.-J. Kim, *Inorg. Chem.*, **36**, 189 (1997).
[6.] J.-H. Choy, J.-B. Yoon, D.-K. Kim, S.-H. Hwang, *Inorg. Chem.*, **34**, 6524 (1995).
[7.] G. Brauer, *Handbook of Preparative Inorganic Chemistry* (Academic Press, New York, 1965), p 1371.
[8.] D. E. Sayers, B. A. Bunker, *X-ray Absorption: Principles, Applications, Techniques of EXAFS, SEXAFS, and XANES*, edited by D. C. Koningsberger, R. Prins, (Wiley-Interscience, New York, 1988), p. 211.
[9.] F. W. Lytle and R. B. Greegor, *Phys. Rev.*, **B37**, 1550, (1988).
[10.] J. Mustre de Leon, J. J. Rehr, S. I. Zabinsky, and R. C. Albers, *Phys. Rev.* **B44**, 4146, (1991).
[11.] S. C. Chang and G. A. Jeffrey, *Acta Cryst.*, **B26**, 673, (1970).
[12.] R. E. Newnham and Y. M. de Haan, *Z Krist.* **117**, 235, (1962).